J Solid State Electrochem (2009) 13:1777–1783
DOI 10.1007/s10008-009-0870-x

ORIGINAL PAPER

Electrodeposition and characterization of Cu-TiO_2 nanocomposite coatings

S. Ramalingam · V. S. Muralidharan · A. Subramania

Received: 17 December 2008 / Revised: 12 May 2009 / Accepted: 18 May 2009 / Published online: 19 June 2009

Abstract Cu-TiO_2 nanocomposites were prepared by electrodeposition method onto copper substrate using an acid copper plating bath containing dispersed nanosized TiO_2. The composition of codeposited TiO_2 nanoparticles in the composite coatings was controlled by the addition of different concentrations of TiO_2 nanoparticles in the bath solution. The average crystallite size was calculated by using X-ray diffraction analysis and it was ~32 nm for electrodeposited copper and ~33 nm for Cu-TiO_2 composite coatings. The crystallite structure was fcc for electrodeposited copper and Cu-TiO_2 nanocomposite coatings. The surface morphology and composition of the nanocomposites were examined by scanning electron microscopy and energy dispersive X-ray spectroscopy analysis. The effect of TiO_2 content on the corrosion and wear resistance properties of the nanocomposite coatings was also presented. The codeposited TiO_2 nanoparticles in the deposit increased the corrosion and wear resistance, which were closely related with TiO_2 content in the nanocomposites. The wear resistance and microhardness of the Cu-TiO_2 nanocomposite coatings were higher than electrodeposited copper. The corrosion resistance property of the electrodeposited copper and Cu-TiO_2 nanocomposite coatings was evaluated by electrochemical impedance and Tafel polarization studies. Cu-TiO_2 composite coatings were more corrosion resistant than electrodeposited copper.

S. Ramalingam · A. Subramania (✉)
Advanced Materials Research Laboratory,
Department of Industrial Chemistry, Alagappa University,
Karaikudi 630 003, India
e-mail: a_subramania@yahoo.co.in

V. S. Muralidharan
Alagappa Chettiar College of Engineering and Technology,
Karaikudi 630 004, India

Keywords Nanocomposites · Electrodeposition of copper · Cu-TiO_2 nanocoating · Composite coatings · Corrosion resistance

Introduction

Nanocomposite coatings refer to electrolysis in which nanosized particles are suspended in an electrolyte and are embedded in the electroformed solid phase, imparting special properties depending on the degree and type of nanoparticle incorporation in the deposit. Electrodeposited composite coatings exhibit enhanced materials properties such as microhardness, wear resistance, and corrosion resistance than the electrodeposited metal coatings [1, 2]. These enhanced properties depend mainly on the nature of the codeposited particles, as well as the distribution of the particles in the metallic matrix [3]. Electrodeposition technique is one of the methods used to fabricate nanocomposite coatings. Many literatures have demonstrated electrodeposited copper- or copper alloy-based nanocomposite materials [4–10]. TiO_2 has many potential applications in various industrial and domestic fields including metallic and organic coatings, catalysis as catalyst support, photovoltaic cells, and wastewater treatment. TiO_2 has also been used to reinforce metallic coatings and it improves wear resistance, hardness, and other properties such as corrosion resistance [11, 12]. TiO_2 codeposition was carried out with Ni, Zn, Ag, and Cu as the metallic components [13–20]. The interest in copper composite coatings has been increased for their potential engineering applications resulting from the outstanding properties of wear resistance, anticorrosion, and self-lubrication. To achieve these properties, various inert particles such as SiC, SiO_2, graphite, Al_2O_3, MoS_2, TiO_2, PTFE, etc. are tried so far [4, 21–27].

Celis et al. reported the kinetics and mechanism of copper-Al_2O_3 nanocomposite coatings [25, 28, 29]. Lozano-Morales et al. studied the effect of Al_2O_3 nanopowder on copper electrodeposition [30]. Benea et al. reported the corrosion behavior of copper and copper matrix composite coatings, with ZrO_2 particles embedded by electrodeposition from an acid copper sulfate plating bath [31]. Yang et al. reported the preparation of single-walled carbon nanotube-reinforced copper composite coatings by electrochemical deposition method [32]. Guo et al. reported the pulse plating of copper-ZrB_2 composite coatings [33].

In this present work, a novel nanostructure metallic composite coatings consisting of nanocrystalline copper matrix (average crystallite size=32 nm) and dispersed titania nanoparticles (average crystallite size=25 nm) have been electrodeposited onto copper substrates from an acid copper sulfate bath. The crystallite size and structure of the electrodeposits were calculated by using X-ray diffraction (XRD) analysis. The surface morphology and composition of copper and Cu-TiO_2 nanocomposite coatings were examined by scanning electron microscopy (SEM) and energy dispersive X-ray spectroscopy (EDAX) analysis. The microhardness and the wear resistance of Cu-TiO_2 nanocomposite coatings were measured by Vickers microhardness tester and Taber abrader tester, respectively. Finally, the corrosion resistance behavior of electrodeposited copper and Cu-TiO_2 nanocomposite coatings was evaluated by electrochemical impedance and Tafel polarization studies.

Experimental methods

Electrodeposition of Cu-TiO_2 nanocomposites

Cu-TiO_2 nanocomposite coatings were electrodeposited from a suspension of TiO_2 nanoparticles in a copper sulfate bath. The optimized bath composition for Cu-TiO_2 composite plating bath was copper sulfate (0.3 M) and sulfuric acid (1.3 M). The TiO_2 nanoparticles (25 nm) were added to the plating bath solution from 25 to 100 g/L with continuous agitation for 4–6 h to ensure uniform dispersion of the nanoparticles in the plating bath [34]. Electrocomposite coatings were carried out using a copper bar of high purity as the anode and polished copper plates of 4.0 cm^2 area as the cathode materials for composite plating. Gelatin (1.0 g/L) was used as an additive in the bath solution. The electroplating parameters such as the current density and pH of the bath were fixed as 5.0 A/dm^2 and 0.2, respectively, at 30 °C. Electrodeposited copper was also obtained under the same condition from an electrolyte without TiO_2 nanoparticles.

Characterizations of Cu-TiO_2 nanocomposites

The crystallite size and structure of the electrodeposited copper and Cu-TiO_2 nanocomposite coatings were measured by XRD analysis. Surface morphology of electrodeposited copper and Cu-TiO_2 nanocomposite coatings was examined by SEM. The composition of the Cu-TiO_2 nanocomposite coatings were measured by EDAX analysis.

The microhardness of the mechanically polished electrodeposited copper and Cu-TiO_2 nanocomposite coatings was measured by Vickers microhardness tester using a load of 50 g for the duration of 15 s. The wear test was conducted on a sliding wear machine of Taber abrader tester with a rotation rate of 1,000 cycles under an applied load of 1 kg.

The corrosion resistance behavior of the electrodeposited copper and Cu-TiO_2 nanocomposite coatings was evaluated by electrochemical impedance spectroscopy. The coated specimen of 1.0 cm^2 area was used as working electrode, the standard calomel electrode (SCE) was used as reference electrode, and the Pt foil acted as a counter electrode. These three electrodes were immersed in 3.5% NaCl solution in a three-electrode cell assembly. The time interval of 10 min was given to attain a steady-state open-circuit potential (OCP) and then the impedance measurements were carried out at the OCP. A sine wave voltage of 10 mV was superimposed on the rest potential. The real part (Z') and the imaginary part (Z'') were measured in the frequency range of 100 kHz to 10 mHz. From the Nyquist plots, the value of charge transfer resistance (R_{ct}) and double layer capacitance (C_{dl}) were measured.

The corrosion resistance behavior of the electrodeposited copper and Cu-TiO_2 nanocomposite coatings of 1.0 cm^2 area was evaluated by Tafel polarization studies. The cell configuration used for this study was same as that used in the impedance measurements. The coated specimen of 1.0 cm^2 area was immersed in 3.5% NaCl solution for the duration of 10 min to attain a steady-state potential. The electrode was then polarized cathodic to anodic direction in the potential range of E_{corr}±250 mV from the OCP at a scan rate of 1 mV/s. The corrosion current densities (i_{corr}) were determined by extrapolating the linear portion of the anodic and cathodic polarization curves. The polarization curves were recorded at least twice to prove the reproducibility of the results. The corrosion rate (CR) was calculated from the corrosion current by using the following equation [35]:

$$\mathrm{CR} = k\left(\frac{i_{\mathrm{corr}}}{\rho}\right)\mathrm{EW}$$

where CR is given in millimeters per year, k=3.27×10^{-3} mm g/μA cm year, ρ=8.96 g/cm^3 is the density of Cu, and EW=31.77 is the equivalent weight of Cu.

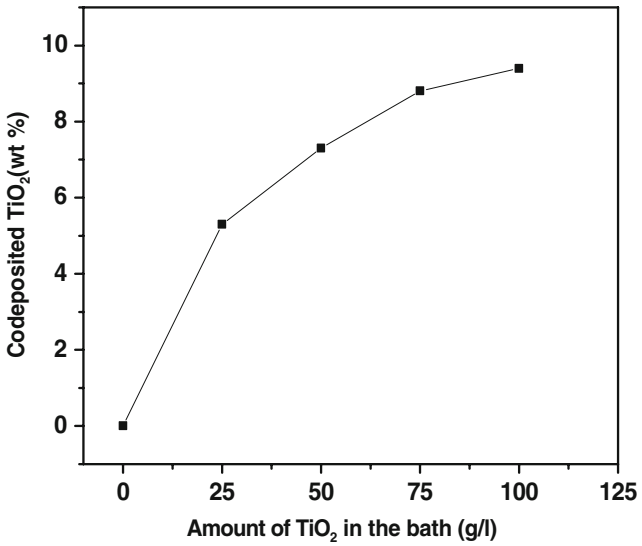

Fig. 1 Effect of amount of TiO_2 in the bath (in grams per liter) on the weight percentage of TiO_2 in the nanocomposite coatings

Results and discussion

Effect of particle concentration

The relationship between the amount of codeposited TiO_2 and the concentration of TiO_2 nanoparticles in the plating bath at the fixed current density of 5.0 A/dm^2 at 30 °C is shown in Fig. 1. The amount of codeposited TiO_2 nanoparticles in the composite coating increased with TiO_2 concentration in the plating bath [2, 3]. The maximum amount of codeposited TiO_2 nanoparticles was achieved at the concentration of 100 g/L of TiO_2. This was confirmed by EDAX compositional analysis. The curve is quite similar to the well-known Langmuir adsorption isotherms, supporting a mechanism based on an adsorption effect. The codeposition of TiO_2 nanoparticles on the cathode surface was suggested by Guglielmi's two-step adsorption model [36, 37]. Once the particles are adsorbed, metal begins building around the cathode slowly, encapsulating, and incorporating the particles. The highest concentration of TiO_2 nanoparticles on the codeposit was due to saturation in adsorption on the cathode surface.

Table 1 EDAX analysis of Cu-TiO_2 (7.3 wt.%) nanocomposite coating obtained from 50 g/L of TiO_2 in the bath

Element	Element %			Average %
	First spot	Second spot	Third spot	
Ti (as TiO_2)	7.30	7.32	7.34	7.32
Cu	92.70	92.68	92.66	92.68

EDAX analysis

A representative EDAX diagram for the Cu-TiO_2 nanocomposite coating obtained by the addition of 50 g/L of TiO_2 nanoparticles is shown in Fig. 2. The EDAX analysis of Cu-TiO_2 nanocomposite coatings gives the average elemental percentage of Ti and Cu as 7.32% and 92.68%, respectively. It confirms the presence of codeposited TiO_2 nanoparticles on the copper matrix (Table 1).

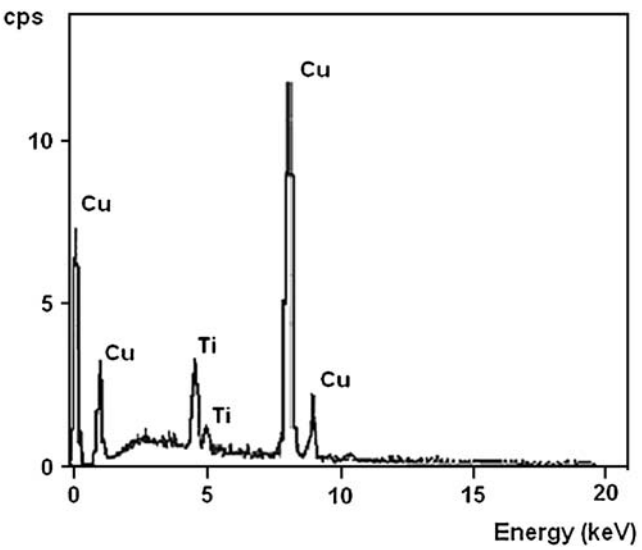

Fig. 2 EDAX analysis spectrum of electrodeposited Cu-TiO_2 nanocomposite coating

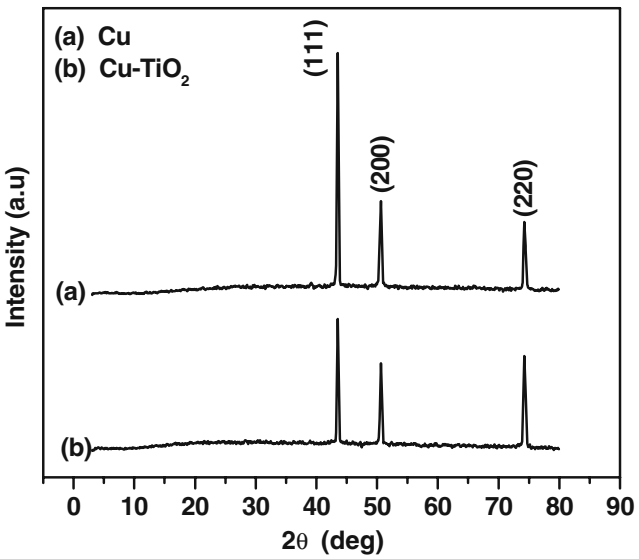

Fig. 3 XRD patterns of both electrodeposited copper and Cu-TiO_2 nanocomposite coatings. **a** Electrodeposited copper, **b** Cu-TiO_2 nanocomposite coating

Table 2 XRD parameters for electrodeposited copper and Cu-TiO_2 nanocomposite coatings

Electro deposits	*d*-spacing (A°)		Miller indices (*h k l*)	Lattice parameter (a)		Str./phase	Average crystallite size (nm)
	Observed	Standard		Observed	Standard		
Copper	2.0794	2.0883	(111)	3.605	3.615	fcc	32
	1.8020	1.8082	(200)				
	1.2763	1.2780	(220)				
Cu-TiO_2 (7.3 wt.%) composite	2.0794	–	(111)	3.605	3.615	fcc	33
	1.8024	–	(200)				
	1.2761	–	(220)				

X-ray diffraction analysis

The crystallite size and structure of the electrodeposited copper and Cu-TiO_2 nanocomposite coatings were calculated by using XRD analysis (Fig. 3). Its corresponding XRD data is given in Table 2. The average crystallite size calculated from the XRD pattern using the Scherrer equation was ~32 nm for copper and ~33 nm for Cu-TiO_2 nanocomposite electrodeposits. The structure of electrodeposited copper and Cu-TiO_2 nanocomposite coatings were crystalline fcc which was confirmed from the JCPDS standards [38], but only noticeable differences in the intensity of (111), (200), and (220) peaks were observed for the Cu-TiO_2 nanocomposite coating compared to electrodeposited copper. The effect of the inclusion of TiO_2 nanoparticles in the copper matrix had only negligible influence on the internal stress, which is evident from the XRD results.

SEM studies

SEM micrographs of the electrodeposited copper and Cu-TiO_2 nanocomposite coatings are shown as Fig. 4. Both the coatings were electrodeposited at a current density of 5.0 A/dm^2 and layer thickness of about

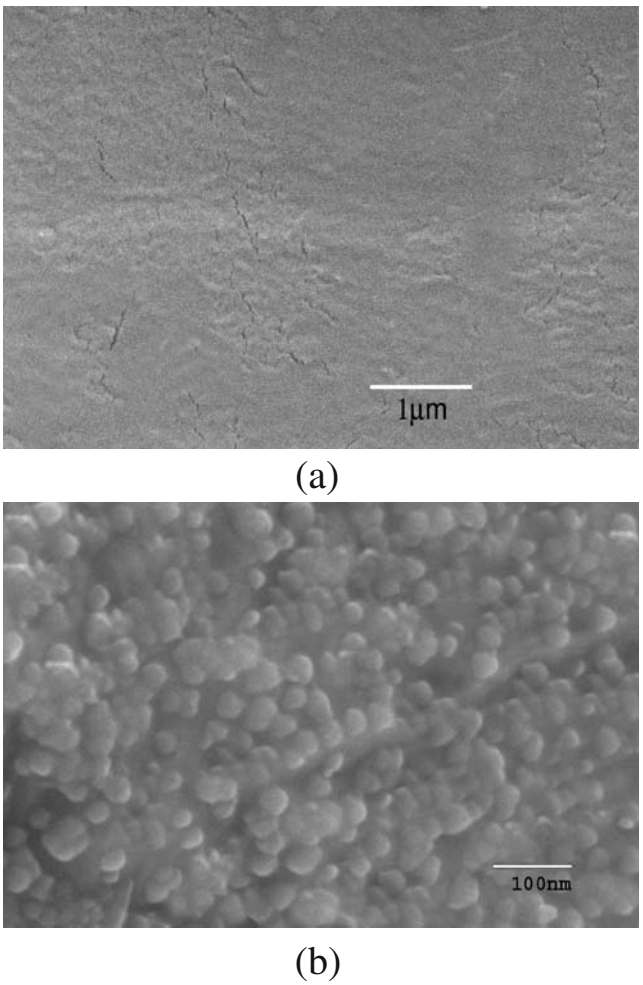

Fig. 4 SEM photographs of electrodeposited copper and Cu-TiO_2 nanocomposite coatings. **a** Electrodeposited copper, **b** Cu-TiO_2 nanocomposite coating

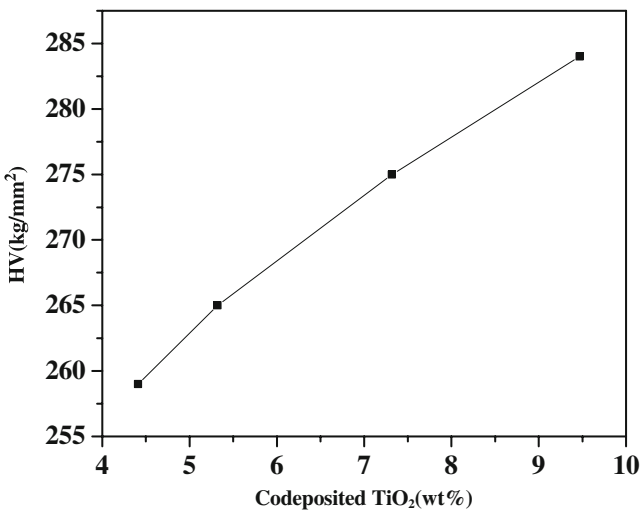

Fig. 5 Effect of the amount of codeposited TiO_2 on the microhardness of Cu-TiO_2 nanocomposite coatings

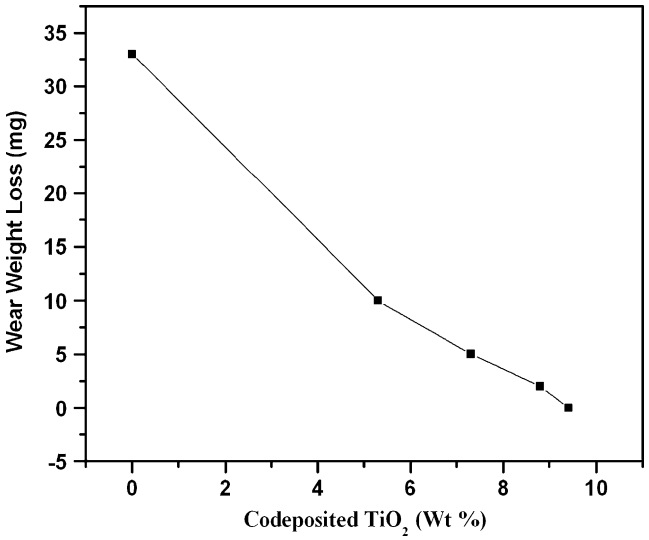

Fig. 6 Effect of the amount of codeposited TiO_2 on the wear weight loss of Cu-TiO_2 nanocomposite coatings

60 μm. The electrodeposited copper showed regular surface and fine crystallites as observed in Fig. 4a and the Cu-TiO_2 nanocomposite coating was more compact than the electrodeposited copper and consisted of smaller and spherical-sized grains as observed in Fig. 4b. It was evident that the TiO_2 nanoparticles were uniformly distributed in the copper matrix by electrodeposition, which was consistent with the EDAX results (Fig. 2). Cu-TiO_2 nanocomposite coatings possessed enhanced mechanical as well as corrosion resistance properties with TiO_2 nanoparticle in the deposit. This is because of the uniform distribution of TiO_2 in the deposit.

Table 3 Impedance parameters for electrodeposited copper and Cu-TiO_2 nanocomposite coatings

Material	TiO_2 (wt.%)	R_{ct} (ohm/cm^2)	C_{dl} (μF/cm^2)
Electrodeposited copper	0	220	72.37
Cu-TiO_2 nanocomposite coatings	5.3	660	24.12
	7.3	850	18.73
	8.8	1,000	15.92
	9.4	1,150	13.84

Microhardness and wear resistance

Vickers microhardness measurements were performed for electrodeposited copper and Cu-TiO_2 nanocomposite coatings as shown in Fig. 5. Microhardness of the Cu-TiO_2 nanocomposite coating was 25 kg/mm^2 higher than that of electrodeposited copper. The microhardness of the nanocomposite coatings increased with TiO_2 particles content in the copper matrix. The enhancement in the hardness of Cu-TiO_2 nanocomposite coatings was due to the strengthening effect caused by the dispersion of TiO_2 nanoparticles in the composite coatings, which impeded the motion of dislocation in the metallic matrix. The Cu-TiO_2 nanocomposite coating exhibited higher hardness values at increased content of the codeposited TiO_2 particles. The improved friction and wear properties were due to the hardened matrix.

The wear resistance of the electrodeposited copper and Cu-TiO_2 nanocomposite coatings were measured by using

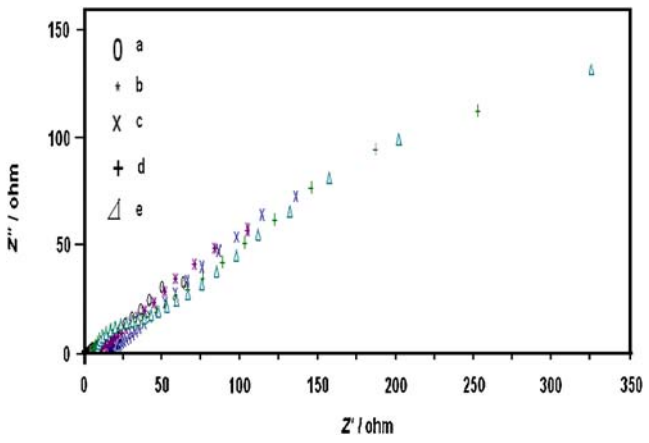

Fig. 7 Impedance plots of electrodeposited copper and Cu-TiO_2 nanocomposite coatings. *a* Electrodeposited copper, *b* Cu-TiO_2 (5.3 wt.%), *c* Cu-TiO_2 (7.3 wt.%), *d* Cu-TiO_2 (8.8 wt.%), *e* Cu-TiO_2 (9.4 wt.%)

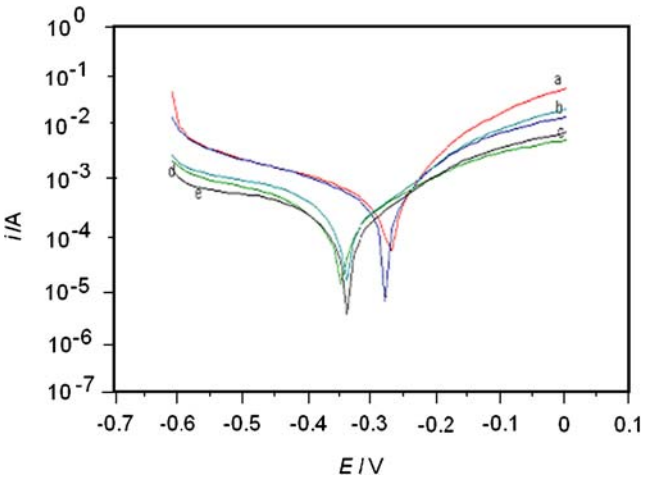

Fig. 8 Tafel polarization plots of electrodeposited copper and Cu-TiO_2 nanocomposite coatings. *a* Electrodeposited copper, *b* Cu-TiO_2 (5.3 wt.%), *c* Cu-TiO_2 (7.3 wt.%), *d* Cu-TiO_2 (8.8 wt.%), *e* Cu-TiO_2 (9.4 wt.%)

Table 4 Tafel polarization parameters for electrodeposited copper and Cu-TiO_2 nanocomposite coatings

Material	TiO_2 (wt.%)	E_{corr} (V) vs SCE	i_{corr} (μA/cm^2)	CR (mm/year)
Electrodeposited copper	0	−0.271	101.6	1.17
Cu-TiO_2 nanocomposite coatings	5.3	−0.286	68.25	0.80
	7.3	−0.343	41.01	0.47
	8.8	−0.338	34.38	0.40
	9.4	−0.339	6.83	0.08

the Taber abrader tester as shown in Fig. 6. From this result, it was found that the Cu-TiO_2 nanocomposite coatings exhibited more wear resistance than electrodeposited copper coating.

Corrosion resistance measurements

Electrochemical impedance studies

Nyquist plots were obtained for the electrodeposited copper and Cu-TiO_2 nanocomposite coatings to get the value of charge transfer resistance (R_{ct}) and double layer capacitance (C_{dl}) as shown in Fig. 7. The charge transfer resistance (R_{ct}) values for Cu-TiO_2 nanocomposite coatings increased and the double layer capacitance (C_{dl}) values decreased with TiO_2 in the composite coatings (Table 3). It revealed that the Cu-TiO_2 nanocomposite coating was more corrosion resistant than electrodeposited copper coating.

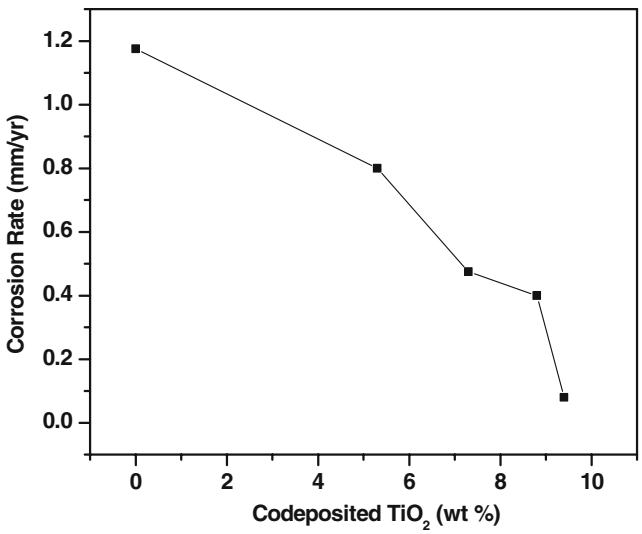

Fig. 9 Dependence of CR on the weight percentage of TiO_2 particles in the Cu-TiO_2 nanocomposite coatings

Polarization measurements

The corrosion potentials (E_{corr}), the corrosion current (i_{corr}), CR, and the Tafel slopes b_a and b_c for copper and Cu-TiO_2 nanocomposite coatings were calculated from the Tafel polarization curves (Fig. 8) and are given in Table 4. It can be seen from the table that the corrosion current (i_{corr}) decreased in all the Cu-TiO_2 nanocomposite coatings compared to electrodeposited copper. The corrosion potential in the case of Cu-TiO_2 nanocomposites had shown a negative shift, confirming the cathodic protective nature of the coatings.

The CR of electrodeposited copper and Cu-TiO_2 nanocomposite coatings was also calculated and the dependence of CR on the weight percent of TiO_2 particles in the Cu-TiO_2 nanocomposite coating is shown in Fig. 9. It revealed that the Cu-TiO_2 nanocomposite coatings (CR=0.08 mm/year) were more corrosion resistant than electrodeposited copper coating (CR=1.175 mm/year) in 3.5% NaCl solution.

Conclusions

The amount of TiO_2 nanoparticles in Cu-TiO_2 nanocomposite coatings increased with the addition of TiO_2 in the plating bath. The average crystallite size calculated was ~32 nm for electrodeposited copper and ~33 nm for Cu-TiO_2 nanocomposite coatings. The structure was crystalline fcc for both electrodeposited copper and Cu-TiO_2 nanocomposite coatings. The microhardness and wear resistance of the Cu-TiO_2 nanocomposite coatings were higher than electrodeposited copper. The charge transfer resistance (R_{ct}) of the Cu-TiO_2 nanocomposite coating was 1.15×10^3 ohm/cm^2, which was higher than that of electrodeposited copper. The Tafel polarization studies showed decreased corrosion currents for all the Cu-TiO_2 nanocomposite coatings than electrodeposited copper coating. The CR of Cu-TiO_2 nanocomposite coatings was less than that of electrodeposited copper coating. It revealed that Cu-TiO_2 nanocomposites were more corrosion resistant than electrodeposited copper in 3.5% NaCl solution.

References

1. Levin BF, Dupont JN, Marder AR (2000) Wear Mater 238:160. doi:10.1016/S0043-1648(99)00363-4
2. Hou KH, Ger MD, Wang LM, Ke ST (2002) Wear 253:994. doi:10.1016/S0043-1648(02)00222-3
3. Wu G, Li N, Zhou D, Mitsuo K (2004) Surf Coat Tech 176:157. doi:10.1016/S0257-8972(03)00739-4
4. Buelens C, Celis JP, Roos JR (1983) J Appl Electrochem 13:541. doi:10.1007/BF00617528
5. Greco VP (1989) Plat Surf Finish 76:68
6. Lee CC, Wan CC (1988) J Electrochem Soc 135:1930. doi:10.1149/1.2096182
7. Chen ES, Lakshmin GR, Sautter FK (1971) Metall Trans 2:937. doi:10.1007/BF02664222
8. Groza JR, Gibeling JC (1993) Mater Sci Eng A 171:115. doi:10.1016/0921-5093(93)90398-X
9. Stojak JL, Talbot JB (2001) J Appl Electrochem 31:559. doi:10.1023/A:1017558430864
10. Li J, Jing J, He H, Sun Y (2002) J Mater Sci Lett 21:939. doi:10.1023/A:1016073606681
11. Fujishima A, Rao TN, Tryk DA (2000) J Photochem Photobiol C. Phytochem Rev 1:1
12. Ito S, Deguchi T, Imai K, Iwasaki M, Tada H (1999) Electrochem Solid-State Lett 2:440. doi:10.1149/1.1390864
13. de Tacconi NR, Boyles AA, Rajeshwar K (2000) Langmuir 16:5665. doi:10.1021/la000037x
14. Deguchi T, Imai K, Matsui H, Iwasaki M, Tada H, Ito S (2001) J Mater Sci 36:4723. doi:10.1023/A:1017927021397
15. Thiemig D, Bund A (2008) Surf Coat Tech 202:2976. doi:10.1016/j.surfcoat.2007.10.035
16. Li J, Sun Y, Sun X, Qiao J (2005) Surf Coat Tech 192:331. doi:10.1016/j.surfcoat.2004.04.082
17. Praveen BM, Venkatesha TV (2008) Appl Surf Sci 254:2418. doi:10.1016/j.apsusc.2007.09.047
18. Gomes A, Silva Pereira MI, Mendon MH, Costa FM (2005) J Solid State Electrochem 9:190. doi:10.1007/s10008-004-0573-2
19. Ramesh CS, Noor Ahmed R, Mujeebu MA, Abdullah MZ (2008) Mater Des (in press)
20. Wan YZ, Wang YL, Tao HM, Cheng GX, Dong XH (1998) J Mater Sci Lett 17:1251. doi:10.1023/A:1006539004598
21. Zhu JH, Liu L, Hu GH, Shen B, Hu WB, Ding WJ (2004) Mater Lett 58:1634. doi:10.1016/j.matlet.2003.08.040
22. Stankovic VD, Gojo M (1996) Surf Coat Tech 81:225. doi:10.1016/0257-8972(95)02486-7
23. Terzieva V, Fransaer J, Celis JP (2000) J Electrochem Soc 147:198. doi:10.1149/1.1393174
24. Ghorbani M, Mazaheri M, Khangholi K, Kharazi Y (2001) Surf Coat Tech 148:71. doi:10.1016/S0257-8972(01)01322-6
25. Celis JP, Roos JR (1977) J Electrochem Soc 124:1508. doi:10.1149/1.2133102
26. Fawzy MH, Ashour MM, Abd El-Halim AM (1995) Trans Inst Metab Finish 73:132
27. Bhalla V, Ramasamy C, Singh N, Pushpavanam M (1995) Plat Surf Finish 82:58
28. Celis JP, Roos JR, Buelens C (1987) J Electrochem Soc 134:1402. doi:10.1149/1.2100680
29. Fransaer J, Celis JP, Roos JR (1992) J Electrochem Soc 139:413. doi:10.1149/1.2069233
30. Lozano-Morales A, Podlaha EJ (2004) J Electrochem Soc 151: C478. doi:10.1149/1.1752934
31. Benea L, Mitoseriu O, Galland J, Wenger F, Ponthiaux P (2000) Mater Corros 51:491. doi:10.1002/1521-4176(200007)51:7<491::AID-MACO491>3.0.CO;2-C
32. Yang YL, Wang YD, Ren Y, He CS, Deng JN, Nan J, Chen JG, Zuo L (2008) Mater Lett 62:47. doi:10.1016/j.matlet.2007.04.086
33. Guo D, Zhang M, Jin Z, Kang R (2006) J Mater Sci Technol 22:514. doi:10.1179/174328406X100680
34. Singh VB, Pandey P (2005) J New Mater Electrochem Syst 8:299
35. Aruna ST, William Grips VK, Rajam KS (2009) J Alloy Comp 468:546. doi:10.1016/j.jallcom.2008.01.058
36. Guglielmi N (1972) J Electrochem Soc 119:1009. doi:10.1149/1.2404383
37. Szczygiel B, Kotodziej M (2005) Trans Inst Metab Finish 83:181. doi:10.1179/002029605X61658
38. Swanson HE, Tatge E (1953) Natl Bur Stand Circulation 1(15):539